Reverse flotation of hematite using a novel bio-collector derived from vitamin E

Rocky Mensah[1,3], Tina Hsia, [2,4], Pouria Amani, [1,3], San H. Thang [2,4], Mahshid Firouzi [1,3,*]

[1] College of Engineering Science and Environment, The University of Newcastle, Callaghan, NSW 2308, Australia
[2] School of Chemistry, Monash University, Clayton, VIC 3800, Australia
[3] ARC Centre of Excellence for Enabling Eco-Efficient Beneficiation of Minerals, The University of Newcastle, Callaghan NSW 2308, Australia.
[4] ARC Centre of Excellence for Enabling Eco-Efficient Beneficiation of Minerals, Monash Node, Monash University Clayton Campus, Australia
* Mahshid.Firouzi@newcastle.edu.au

Abstract

Reverse anionic flotation of hematite–silica mixtures was assessed at laboratory scale using a novel bio-based collector, vitamin E sodium succinate (VE_SS). A synthetic feed containing 30 wt% hematite and 70 wt% silica was prepared from mined, well-characterised sources (hematite ~93.6 wt% Fe_2O_3; silica ~97.8 wt% SiO_2). With $CaCl_2$ as quartz activator and soluble starch as hematite depressant, VE_SS achieved more than 95% hematite recovery to the hematite-rich concentrate and ~7.7% silica recovery to the concentrate (≈92% silica rejection) in a single rougher stage, yielding a rougher concentrate of ~55 wt% Fe and ~19–20 wt% SiO_2 for this tailings-like feed (separation efficiency ~90%; selectivity index 21.9). Surface characterisation by zeta potential, contact angle and FTIR measurements indicated strong VE_SS adsorption on Ca^{2+}-activated quartz at higher pH, consistent with increased surface hydrophobicity and the observed selectivity. Overall, VE_SS shows practical potential as a bio-based collector for reverse anionic flotation of hematite.

Keywords: Vitamin E sodium succinate, Bio-based collector, Reverse anionic flotation, Hematite beneficiation, Quartz activation.

1 Introduction

Iron and steel account for about 95% of global metal tonnage and underpin industrialisation. Australia is a leading producer and holds about 28% of the world's estimated iron reserves.

Iron ores are generally classified as high-grade (direct shipping ores, DSO) or low-grade. While the hematite and magnetite contain 69.94% and 72% Fe, respectively, many hematite-bearing ores (and processing residues) contain substantially less Fe and higher silicate content, necessitating upgrading. As high-grade resources decline, the processing of lower-grade and complex feeds has increased, heightening the need for efficient beneficiation.

Flotation is a well-established physico-chemical separation process that exploits differences in surface wettability using surface-active reagents (depressants, activators, frothers, collectors) to tune selectivity and kinetics (Fuerstenau & Healy, 1972).

In iron processing, flotation is either direct (iron floated) or reverse (iron depressed). Reverse flotation is commonly used to remove gangue (mainly silicates) by floating impurities while depressing iron. Extensive studies have been conducted on reagent optimization in reverse flotation of iron ores to improve separation performance (Araujo et al., 2005; Filippov et al., 2014; Nakhaei & Irannajad, 2018).

Two primary types of collectors are employed in iron ore flotation, anionic and cationic collectors. Anionic collectors typically consist of hydrocarbons combined with alkali salts of straight-chain fatty acids or alkyl aryl sulfonates. In contrast, cationic collectors generally contain a hydrocarbon group along with salts of bases, most often chlorides or acetates (Sahoo et al., 2015). While reverse cationic flotation offers the advantage of faster flotation rates, it is more sensitive to slime contamination, which can hinder the flotation process, and its collectors are relatively costly compared to anionic alternatives. Considering these limitations, reverse anionic flotation has emerged as one of the most widely adopted and cost-effective technologies for the efficient utilization of iron ore resources (Filippov et al., 2014; Nakhaei & Irannajad, 2018).

In anionic reverse flotation, iron is first rendered hydrophilic using depressants, quartz is then activated, and finally anionic collectors are used to float the activated gangue into the froth phase as tailings, leaving the depressed iron in the cell as concentrate. Typical depressants include starch, carboxy methyl cellulose (Turrer & Peres, 2010), tannis and their derivatives (Tohry et al., 2021), and locus bean gum (Kordloo et al., 2023). Starch that is composed of glucose polymers amylopectin and amylose, is widely used because of its availability, cost-effectiveness and effectiveness as a hematite depressant (Rath & Sahoo, 2022). Studies using thermal analysis, FTIR and zeta potential measurements suggest starch preferentially adsorbs on hematite due to abundant hydroxylated metal adsorption sites (Weissenborn et al., 1994,

1995). Kar et al. (2013) compared soluble, corn, potato, and rice starches for hematite and reported soluble starch to be the most effective depressant for hematite.

Quartz typically carries a negative surface across most pH values, producing electrostatic repulsion with anionic collectors (Parks, 1965). Activation by multivalent cations (such as Ca^{2+}, $Mg^{2+,}$ Pb^{2+}, Zn^{2+}, Cu^{2+}, Ni^{2+}, Fe^{3+}) can adsorb onto the silica surface, modify its charge and promote anionic collector adsorption and flotation (Ding et al., 2023; Ejtemaei et al., 2012; Fornasiero & Ralston, 2005; Jie et al., 2014). Calcium activation, for instance, is pH-dependent and is often most effective at alkaline pH (~11-12) for promoting collector adsorption (Ding et al., 2023; Fuerstenau & Cummins, 1967; Kou et al., 2016; Ozkan et al., 2009).

Fatty acids and their salts (e.g., sodium oleate) are common collectors for activated silica due to their cost, effectiveness, and relatively low environmental impact (Kou et al., 2016; Luo et al., 2016). Limitations of conventional fatty-acid collectors such as low solubility at low temperatures (Bagby et al., 2000; Quast, 2006) have motivated the development of modified and bio-based collectors with improved solubility, activity and selectivity (Cao et al., 2013). Examples include α-brominated fatty acids (α-BLA, α-BDA) synthesised from lauric and decanoic acids, which show improved quartz recovery at low temperatures and reduced sensitivity to pulp temperature (Luo et al., 2015; Zhu et al., 2015). Amide-modified fatty acid collectors such as 2-(carbamoylamino)lauric acid (2-CLA) have demonstrated stronger chemisorption and hydrogen-bonding interactions on activated quartz and improved performance relative to lauric acid (Guo et al., 2020). Fang et al. (2021) investigated the use of a novel collector, (E)-8,11-dihydroperoxyoctadec-9-enoic acid, EDEA, which was synthesized from the oxidation of fatty acid at low temperatures. This collector showed a stronger affinity for quartz than hematite and magnetite under reverse flotation conditions, achieving an excess of about 30% recovery of quartz at the same concentration of oleic acid for single minerals flotation. Bench scale flotation tests revealed EDEA outperformed oleic acid at low flotation temperature. Amphoteric collectors (e.g., LDEA) and amino-acid based surfactants (e.g., lauroyl lysine) have also been proposed, showing good quartz selectivity, lower required dosages and improved low-temperature performance in laboratory tests (Luo et al., 2018, 2019, 2021; Wu et al., 2024).

Most new collectors for the reverse flotation of iron ore have been evaluated in single-mineral systems, typically focusing on quartz. While these studies elucidate adsorption behaviour, they do not capture the competitive interactions that arise in mixed mineral systems. Studies on

mixed mineral systems, on the other hand, involve complex flotation cycles. Therefore, investigating collector performance in a binary or multi-mineral-simple flotation system is essential for assessing its practical applicability.

In our previous work, we synthesised a bio-based collector, Vitamin E sodium succinate (VE_SS) and compared its adsorption behaviour with sodium oleate on single minerals (hematite and quartz) using zeta potential, contact angle, FTIR and XPS, showing VE_SS to be effective across a broad pH range (Mensah et al., 2025). Here we bridge the single- to mixed-mineral gap by evaluating VE-SS in reverse flotation under a realistic reagent regime ($CaCl_2$ activation of quartz, soluble starch depression of hematite). A controlled binary mixture (30 wt% hematite, 70 wt% silica) was employed as a model tailings system. This simplified mixture does not reproduce the full mineralogical complexity of plant tailings, but it provides a reproducible platform to quantify practical selectivity (grade–recovery, silica rejection, separation efficiency, selectivity index) in a single-stage operation. This study presents the first mixed-mineral reverse flotation evaluation of VE_SS, establishing its separation performance beyond single-mineral tests and providing a controlled protocol to inform subsequent circuit staging and plant-scale trials.

2 Materials and methodology

2.1 Materials and Reagents

The hematite sample was received from a commercial mine and 200G size silica sample was sourced from Holcim. The results of X-ray Fluorescence (XRF) analysis of the pure minerals, performed using Bruker S8 TIGER series II, are presented in Table 1 and Table 2.

Soluble starch was purchased from Chem Supply and used as a hematite depressant. $CaCl_2$ was used as an activator for silica, and Vitamin E sodium succinate (VE_SS) was derived from the natural product α-tocopherol commonly known as vitamin E was used as a collector. VE_SS is the sodium salt of D-α-tocopherol succinate, prepared by succinylation of D-α-tocopherol followed by neutralisation with NaOH. Full synthetic details and characterisation are reported in (Mensah et al., 2025). The structure of VE_SS is illustrated in Figure 1.

Sodium hydroxide (NaOH) and hydrochloric acid (HCl) were used as pH modifiers and NaCl was used as a background electrolyte for particle surface charge measurements. Milli-Q water with a resistivity of 18 mΩ/cm was used for all the experiments.

Table 1. Elemental analyses of hematite (wt%)

Component	Al_2O_3 (%)	SiO_2 (%)	P_2O_5 (%)	SO_3 (%)	Cl (%)	CaO (%)	Fe_2O_3 (%)
Concentration	0.697	4.742	0.339	0.101	0.143	0.222	93.560

Table 2. Elemental analyses of silica (wt%)

Component	Al_2O_3 (%)	SiO_2 (%)	P_2O_5 (%)	Cl (%)	CaO (%)	Fe_2O_3 (%)
Concentration	1.148	97.769	0.433	0.220	0.122	0.258

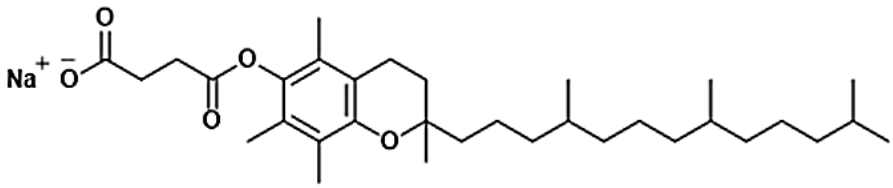

Figure 1 Structure of vitamin E sodium succinate (VE_SS).

2.2 Micro-flotation experiments

A single-stage reverse flotation was conducted at room temperature using a modified 250 mL mechanical flotation cell to evaluate the performance of VE_SS. A binary feed sample, comprising of 70% silica and 30% hematite (total iron grade (TFe) of 19.63), was initially mixed with Milli-Q water to create a 6 wt.% pulp in the flotation cell, operated at an impeller speed of 840 rpm for one minute. The pulp pH was adjusted to 11.5 using NaOH and HCl as pH modifiers and monitored with a TPS digital pH meter (TPS Pty. Ltd., Springwood, Qld., Australia). Reagents were added every five minutes in the following sequence: depressant (soluble starch), activator ($CaCl_2$), and collector (VE_SS). The pH was carefully monitored and controlled throughout the conditioning period using the pH modifiers and pH meter.

Hematite surfaces were depressed using soluble starch, an effective reagent for rendering hematite hydrophilic (Kar et al., 2013). Silica particles were activated with Ca^{2+} to promote VE_SS adsorption onto the gangue. Based on preliminary optimization, all flotation experiments were conducted with 2000 ppm soluble starch, which provided the strongest depression of hematite, and 100 ppm Ca^{2+}, which gave the most effective quartz activation. The pH was fixed at 11.5, as calcium activation is known to be most efficient under alkaline conditions (~11–12), thereby enhancing collector adsorption (Ding et al., 2023; Fuerstenau & Cummins, 1967; Kou et al., 2016; Ozkan et al., 2009).

Flotation was performed for five minutes with an airflow rate of 3 litres per minute, and tailings samples were collected using an automated froth scraper. Silica was enriched in the froth as tailings, leaving hematite in the cell, which was collected as concentrate samples. Each test was repeated multiple times to ensure data reliability. Concentrate and tailings samples were dried in an oven and processed for further analysis. Chemical analysis via X-ray fluorescence was conducted on each sample stream to determine the hematite and silica assay values for further calculations. The flowsheet of the micro-flotation test is represented in Figure 2. To provide further insights into the efficiency of the separation process, a geometric mean, known as the Gaudin selectivity index (SI), as defined in Equation 1 (Gaudin, 1939), was used to determine the relative recoveries and rejections of the binary feed. Additionally, a simple key metric known as separation efficiency (SE) was also used to quantify the effectiveness of the flotation. As shown in equation 2, the SE concept is visualized as the difference between the recoveries of the valuable minerals and the gangue in the concentrate. Thus, the higher the SE and SI values, the better the separation (Irannajad et al., 2018; Wills & Finch, 2015).

$$SI = \sqrt{\frac{R_h \times J_q}{(100 - R_h) \times (100 - J_q)}} \quad (1)$$

where R_h and J_q are the recoveries of hematite in the concentrate and quartz in the tailings respectively.

$$SE = R_h - R_q \quad (22)$$

where R_h and R_q are the recoveries of hematite and quartz in the concentrate.

All experiments were conducted at a fixed temperature of 20 °C.

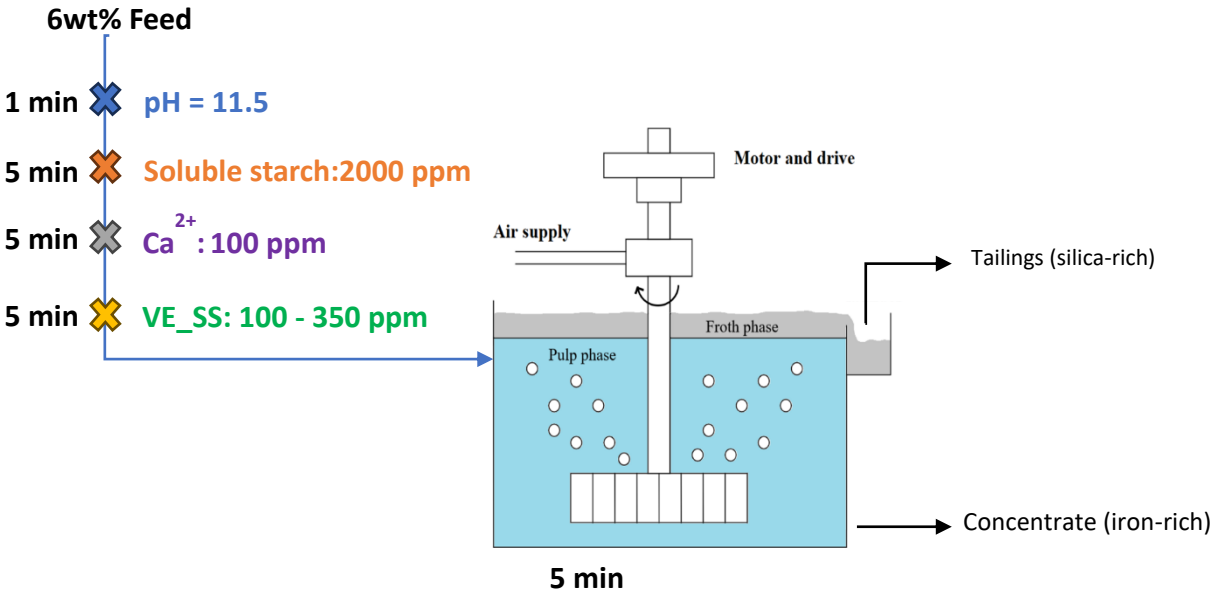

Figure 2 Flowsheet of the flotation tests

2.3 Zeta potential measurement

Zeta potential measurements of hematite and silica, before and after reagent treatment, were carried out using a Malvern Zetasizer Pro. The pulp pH was adjusted with sodium hydroxide or hydrochloric acid. For each test, approximately 30 mg of the pure material (<38 µm) was suspended in 80 ml of 1.0 mM NaCl background solution and dispersed using a magnetic stirrer. Reagents were then added sequentially, following the order of the flotation process. After the conditioning period, the solution was allowed to settle, and the supernatant of the mixture was collected for zeta potential measurements. Measurements were conducted at a constant temperature, both in the presence and absence of predetermined reagent concentrations, where required. Each reported value represents the average of at least three replicates, with a maximum deviation of ± 3mV.

To isolate the direct effect of each reagent on an individual mineral's surface charge, zeta-potential measurements were performed on single-mineral suspensions. Instead of using the total dosages applied in flotation, the tests employed concentrations approximating the residual reagent levels expected in solution after adsorption onto the target mineral. This approach allowed assessment of how adsorbed and residual amounts of each reagent influence the target and non-target mineral, respectively, under conditions comparable to flotation.

2.4 Contact angle measurement

To characterize the surface wettability of mineral samples, contact angle measurements were performed using the sessile drop method with an Optical Contact Angle device (OCA 25L-PMC; DataPhysics Instruments GmbH, Germany). Mineral samples were first conditioned with the appropriate reagents at the desired pH to replicate flotation conditions. After conditioning, the samples were filtered using a vacuum filter to remove excess liquid and the residues were then dried in an oven set to 60°C for one hour to eliminate moisture. The dried samples were then compressed into uniform tablets using a hydraulic press to provide a flat consistent surface suitable for contact angle analysis. Contact angles were measured on these compressed tablets under the specified conditions. A detailed procedure is described by Wright et al. (2025).

2.5 Fourier transform infrared spectroscopy analysis

Fourier transform infrared spectroscopy (FTIR) analysis was performed using an Agilent Carey 650 FTIR to characterise the functional groups of the sample within the 650 – 4000 nm wavelength range. Sample preparation involved mixing 0.5 g of mineral with 50 mL of distilled water. For silica analysis, 550 mg/L of calcium chloride was added, followed by 500 mg/L of VE_SS. For hematite analysis, 4000 mg/L of starch was added, with or without the addition of 100 mg/L of VE_SS, for comparative analysis. All mixtures were adjusted to pH 11.5 and stirred at room temperature for 30 minutes. The suspensions were then filtered, and the residues were thoroughly washed with distilled water. Pure samples of VE_SS, starch and minerals were prepared under the same conditions and used as controls. All samples were dried overnight in a vacuum oven before FTIR spectrum measurements.

3 Results and discussion

3.1 Zeta potential measurements

Zeta-potential measurements on single-mineral suspensions were conducted at solution concentrations selected to mirror the mixed-mineral flotation conditions. For the target mineral, reagent levels corresponded to the flotation-optimal concentrations of the reagents that act on that mineral; for the non-target mineral, reagent levels approximated the residual concentrations expected in the pulp after preferential adsorption in the mixed system. Accordingly, silica tests included calcium activator and collector at flotation-relevant levels together with a background level of soluble starch representative of the portion remaining in solution when starch predominantly adsorbs on hematite. Hematite tests included soluble starch at its flotation-relevant level together with a background level of collector representative of the portion remaining in solution after uptake on Ca-activated silica. All measurements were performed at the same pH and ionic strength as flotation, with conditioning, rinsing and measurement protocols described previously. Control measurements without reagents and with individual reagents were also obtained to verify trends.

Considering the above methodology, the zeta potential measurements of silica and hematite in the presence and absence of reagents are shown in Figure3Figure3 3. For silica, the surface was negatively charged across the tested pH range, with a notable increase in zeta potential values above pH 10. This behaviour agrees with previous reports (Cao et al., 2013; Fang et al., 2021), and is attributed to the dissociation of -Si-OH to -Si-O^- sites and hydration of silanol groups, which increase surface negativity with rising OH^- concentration. At pH>10, however, OH^- saturation creates a shielding effect, reducing surface charge density and thus increasing the measured zeta potential. Conditioning silica with VE_SS alone produced no significant changes, indicating minimal adsorption of the collector.

In contrast, $CaCl_2$ conditioning increased the zeta potential of silica, particularly under alkaline conditions (pH>10), rendering the surface less negatively charged. This agrees with the known good floatability of $CaCl_2$-activated quartz under alkaline conditions. Adsorption of Ca^{2+} and $Ca(OH)^+$ onto the quartz surface occurs through electrostatic interactions (Zhang et al., 2023), providing active sites for subsequent VE_SS adsorption. The enhanced activation under alkaline conditions can be attributed to the preferential adsorption of $Ca(OH)^+$. According to

the calcium speciation diagram at 10^{-3} mol/L (Ozkan et al., 2009), Ca^{2+} dominates below pH 10, whereas $Ca(OH)^{+}$ becomes increasingly important above this threshold due to hydroxide ion abundance. Specific adsorption of $Ca(OH)^{+}$ on negatively charged silica sites reduces electrostatic repulsion, facilitating collector adsorption. Consistently, VE_SS adsorption on Ca^{2+}-activated quartz was evident across the entire pH range, but was markedly stronger at pH >10. The presence of soluble starch, however, did not significantly alter the zeta potential of VE_SS-conditioned quartz.

For hematite, the zeta potential as a function of pH is shown in Figure3Figure3 3b**Error! Reference source not found.**. It is seen that the surface charge of hematite particles decreases with increasing pH, with an isoelectric point (IEP) around pH 5. Exposure to VE_SS led to a further decrease in zeta potential, indicating adsorption of VE_SS on hematite particles.

The addition of soluble starch also decreased the zeta potential and shifted the IEP toward more acidic values, confirming starch adsorption on the hematite surface. Notably, subsequent introduction of VE_SS caused no significant change in the zeta potential of starch-treated hematite, demonstrating that starch effectively blocked VE_SS interaction with hematite.

Calcium chloride was also found to influence the zeta potential and VE_SS adsorption behaviour. Below the IEP, hematite carried a positive charge, limiting Ca^{2+} adsorption. Above the IEP, the surface became increasingly negative with rising pH, which promoted Ca^{2+} adsorption and corresponded to an increase in zeta potential in the presence of Ca^{2+}. Similarly, Ca^{2+} had little effect on VE_SS adsorption below the IEP but produced a distinct shift in surface charge above the IEP, suggesting co-adsorption of VE_SS and Ca^{2+} on hematite surfaces under alkaline conditions.

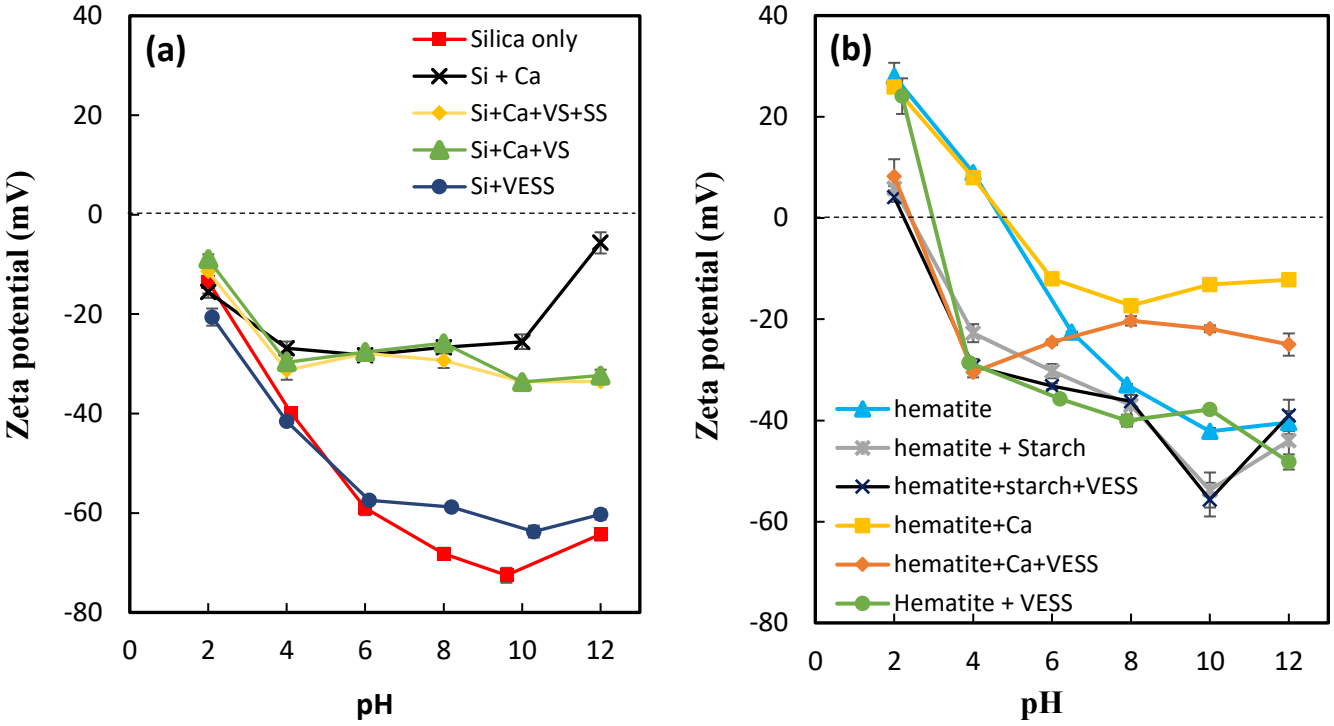

Figure3 3 Zeta potential of (a) quartz and (b) hematite in the presence of different reagents as a function of pH

3.2 Contact angle measurements

The contact angle of silica was measured in the presence and absence of Ca^{2+} and VE_SS at a fixed pH of 11.5, as shown in Figure 4 Figure 44a. Silica is inherently hydrophilic, with a contact angle of 27 ± 5°. In the absence of Ca^{2+}, VE_SS showed minimal adsorption onto silica, with the contact angle remaining approximately 27 ± 5°. However, upon addition of 100 ppm Ca^{2+}, VE_SS adsorption was significantly enhanced, resulting in a high contact angle of ~80° and, consequently, increased hydrophobicity of the Ca^{2+}-activated quartz.

The pH dependence of quartz wettability in the presence of Ca^{2+} and VE_SS was also investigated Figure 4 Figure 44b. The data show that the contact angle increased steadily with pH, from 36.9 ± 2° at pH 2 to 82 ± 7° at pH 12. This trend indicates that VE_SS adsorption on Ca^{2+}-activated quartz becomes progressively stronger at higher pH, leading to enhanced hydrophobicity under alkaline conditions. These observations are consistent with previous reports on the improved effectiveness of calcium activation at high pH (Ding et al., 2023; Fuerstenau & Cummins, 1967; Kou et al., 2016; Ozkan et al., 2009), and they support conducting the micro-flotation experiments at the chosen optimum pH of 11.5.

Figure 4Figure 44c presents contact angle values of hematite in the presence and absence of VE_SS and starch at a fixed pH of 11.5. To better illustrate the depressing effect of starch, experiments were conducted at 250 ppm VE_SS, assuming full collector availability for adsorption onto hematite surfaces. The results show that hematite has a contact angle of 42.7 ± 0.5°. Conditioning with VE_SS in the absence of starch increased the contact angle to 102.5 ± 5.1°, indicating strong adsorption of VE_SS on hematite, enhancing its hydrophobicity. In contrast, pre-treatment with soluble starch before VE_SS lowered the contact angle to 33.7 ± 1.3 ° and minimised VE_SS adsorption so that hematite maintained its hydrophilic character in the presence of VE_SS. These results demonstrate that starch effectively inhibits VE_SS adsorption, making its addition essential for achieving high separation efficiency in the reverse flotation of hematite.

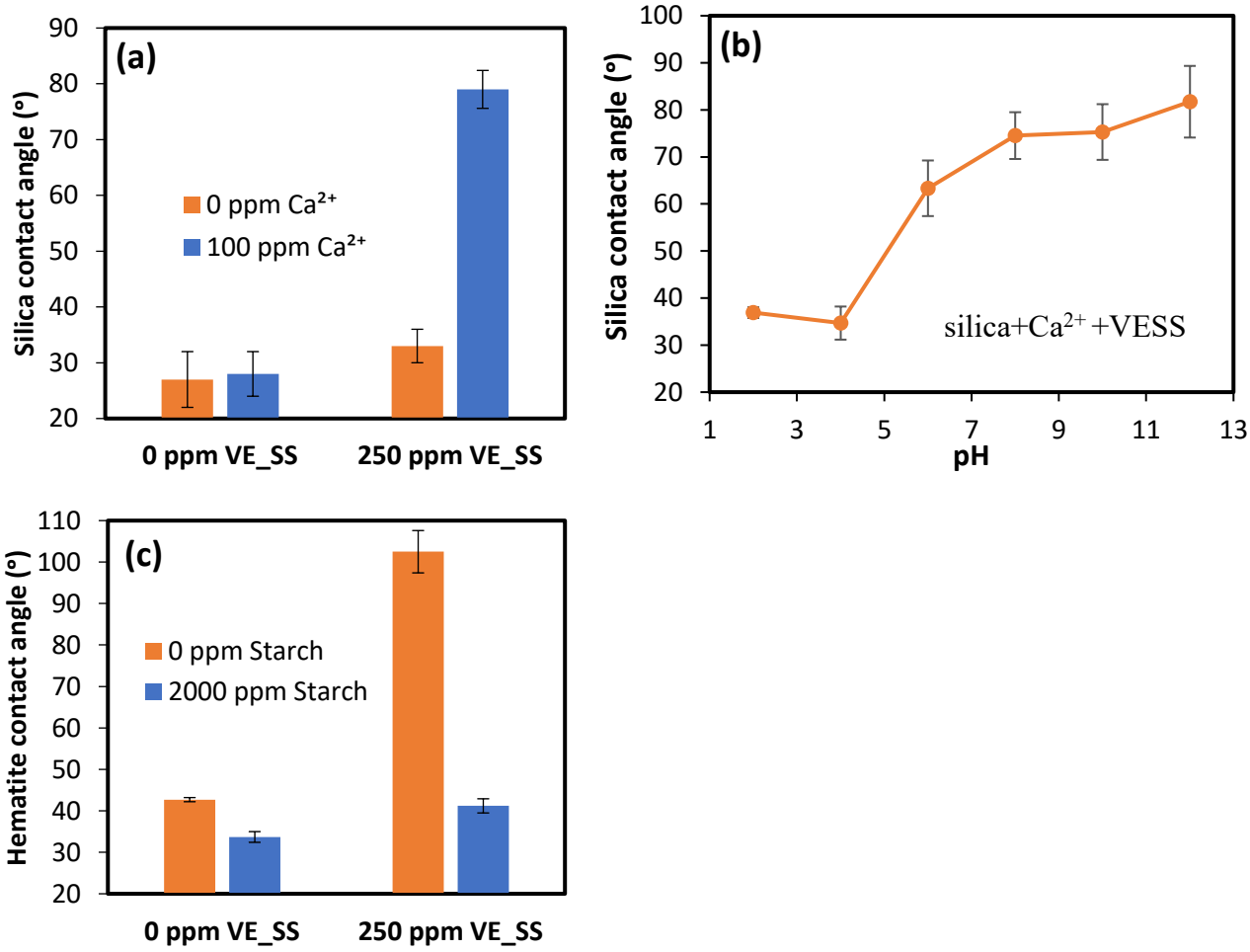

Figure 44 Contact angle of (a) silica in the absence and presence of Ca^{2+} and VE_SS at fixed pH = 11.5, (b) activated silica and VE_SS as a function of pH, and (c)hematite in the absence and presence of starch and VE_SS at fixed pH = 11.5.

3.3 FTIR analysis

FTIR spectroscopy was employed to investigate the adsorption behaviour of VE_SS on silica and hematite surfaces, with $CaCl_2$ used as the activator for silica and starch as the depressant for hematite. The corresponding spectra are presented in Figure 55Figure 5.

VE_SS exhibits distinct –CH stretching bands between 2800 and 3000 cm^{-1}, along with a carboxylate asymmetric stretch near 1567 cm^{-1}. For calcium-activated silica (Figure 5a), these collector-related peaks were clearly observed in samples treated with VE_SS, confirming adsorption. In contrast, such peaks were absent on silica without calcium activation (bare silica) exposed to VE_SS, our previous work Mensah et al. (2025), reported adsorption of VE_SS on hematite surfaces.

The FTIR spectra of starch (Figure 5Figure 55b) showed a broad –OH stretching band around 3300 cm^{-1}, characteristic of polysaccharide hydroxyl groups. A similar feature was detected for hematite treated with starch, confirming its adsorption onto the mineral surface. When VE_SS was subsequently introduced (Figure 5Figure 55c), no distinct collector peaks appeared, indicating that pre-adsorbed starch effectively blocked the hematite surface and prevented VE_SS interaction.

This inhibition is consistent with the effective separation of hematite from silica observed in the reverse micro flotation experiments, presented in the following section. Overall, the FTIR spectra provides spectroscopic evidence consistent with selective adsorption; VE_SS adsorbs on Ca-activated silica, while pre-adsorbed starch passivates hematite, reinforcing its role as a depressant.

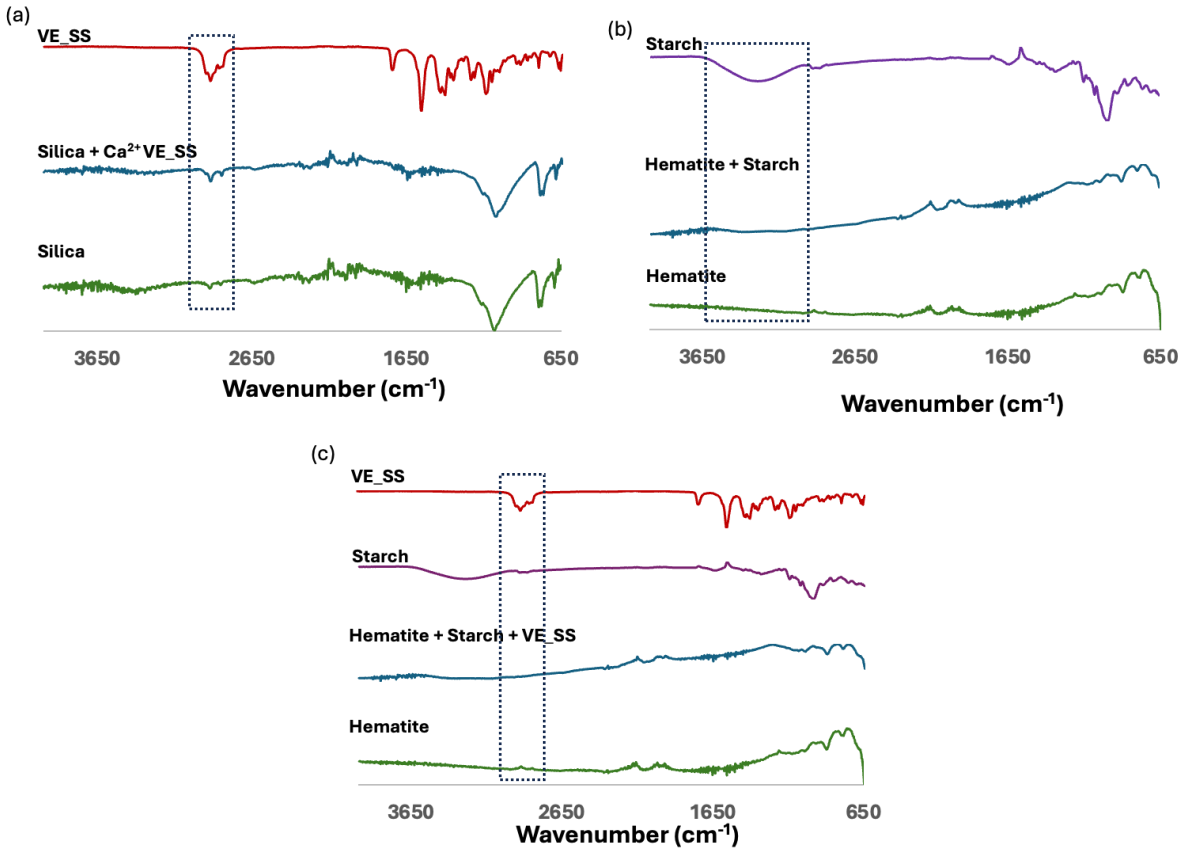

Figure 55 FTIR of (a) Silica surface in the presence of $CaCl_2$ and VE_SS, (b) Hematite surface in the presence of starch and (c) Hematite surface in the presence of starch and VE_SS at pH 11.5

3.4 Micro-flotation

The single-stage flotation performance of hematite-quartz mixture (30:70 ratio) under fixed reagent concentrations- 2000 ppm soluble starch and 100 ppm Ca^{2+} at pH 11.5 is shown in Figure 6. The figure reports the hematite and silica recoveries and the total iron grade as functions of VE_SS dosage. Hematite recovery to the concentrate remained >95% across all VE_SS dosages, consistent with effective starch depression: by rendering hematite surfaces hydrophilic, starch inhibited VE_SS adsorption and kept hematite in the non-floated product. Silica recovery to the concentrate decreased with increasing VE_SS to a minimum at the optimum dose (≈7.7%; ≈92% rejection), which coincided with a maximum in total iron grade. The underlying surface interactions are examined in Sections 3.2–3.4 (zeta potential, FTIR and contact angle).

Increasing VE_SS reduced quartz reporting to the concentrate and improved the concentrate grade, reaching a minimum silica recovery of ~7.7% at 250 ppm VE_SS. Increasing the

collector further to 350 ppm raised silica recovery to ~9.8% and lowered the concentrate grade by ~3%. The optimum collector dosage was therefore taken as 250 ppm, yielding a selectivity index of 21.89 (Equation 1). Under these conditions, total iron (TFe) increased from 19.63 wt% in the feed to 55.34 wt% in the concentrate in a single rougher stage, with an overall separation efficiency (Equation 2) of approximately 90%.

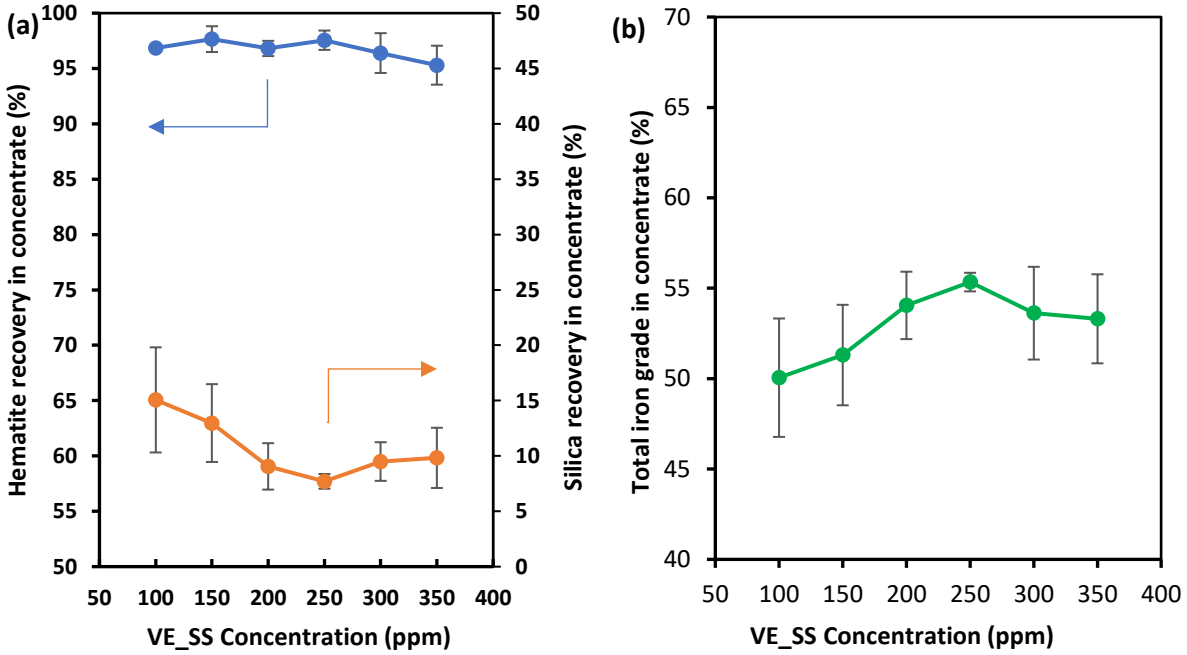

Figure 6 (a) Hematite and silica recoveries to the concentrate; (b) total iron grade in the concentrate versus VE_SS concentration.

4 Conclusions

This study demonstrates the potential of Vitamin E Succinate (VE_SS) as a sustainable bio-based collector for the reverse flotation of hematite. Building on earlier work where VE_SS was benchmarked against sodium oleate in single-mineral and direct-flotation systems, the present study evaluated its performance under realistic reverse-flotation conditions.

In single-stage rougher tests using a 30 wt% hematite–70 wt% silica feed, VE_SS achieved hematite recoveries exceeding 95%, with the total iron grade increasing from 19.6 % in the feed to 55.3 % in the concentrate. A selectivity index of 21.8 and a separation efficiency of 90 % confirmed good single-stage selectivity, while soluble starch effectively depressed hematite to maintain separation. Although the concentrate grade is not at product specification, this performance demonstrates strong separation capability in a single stage. Further improvements

in grade and recovery would be expected through additional cleaner and scavenger stages, which were beyond the scope of this study.

Surface analyses provided insight into the adsorption mechanism of VE_SS. Contact-angle, zeta-potential and FTIR measurements all indicated negligible adsorption on silica without calcium activation, but strong adsorption on Ca-activated silica, particularly under alkaline conditions. consistent with the increased surface hydrophobicity observed.

5 Acknowledgements

The authors acknowledge the funding support from the Australian Research Council for the ARC Centre of Excellence for Enabling Eco-Efficient Beneficiation of Minerals, grant number CE200100009.

References

Araujo, A. C., Viana, P. R. M., & Peres, A. E. C. (2005). Reagents in iron ores flotation. *Minerals Engineering*, *18*(2), 219-224. https://doi.org/https://doi.org/10.1016/j.mineng.2004.08.023

Bagby, M., Johnson Jr, R., Daniels, R., Contrell, R. R., Sauer, E., Keenan, M., Krevalis, M., & Staff, U. B. (2000). Carboxylic acids. *Kirk‐Othmer Encyclopedia of Chemical Technology*.

Bulayani, M. M., Raghupatruni, P., Mamvura, T., & Danha, G. (2024). Exploring low-grade iron ore beneficiation techniques: a comprehensive review. *Minerals*, *14*(8), 796.

Cao, Z., Zhang, Y., & Cao, Y. (2013). Reverse flotation of quartz from magnetite ore with modified sodium oleate. *Mineral Processing and Extractive Metallurgy Review*, *34*(5), 320-330.

Ding, Z., Li, J., Yuan, J., Yu, A., Wen, S., & Bai, S. (2023). Insights into the influence of calcium ions on the adsorption behavior of sodium oleate and its response to flotation of quartz: FT-IR, XPS and AMF studies. *Minerals Engineering*, *204*, 108437. https://doi.org/https://doi.org/10.1016/j.mineng.2023.108437

Ejtemaei, M., Irannajad, M., & Gharabaghi, M. (2012). Role of dissolved mineral species in selective flotation of smithsonite from quartz using oleate as collector. *International Journal of Mineral Processing*, *114-117*, 40-47. https://doi.org/https://doi.org/10.1016/j.minpro.2012.09.004

Fang, J., Ge, Y., Liu, S., Yu, J., & Liu, C. (2021). Investigations on a novel collector for anionic reverse flotation separation of quartz from iron ores. *Physicochemical Problems of Mineral Processing*, *57*(1), 136-155. https://doi.org/https://doi.org/10.37190/ppmp/130472

Filippov, L. O., Severov, V. V., & Filippova, I. V. (2014). An overview of the beneficiation of iron ores via reverse cationic flotation. *International Journal of Mineral Processing*, *127*, 62-69. https://doi.org/https://doi.org/10.1016/j.minpro.2014.01.002

Fornasiero, D., & Ralston, J. (2005). Cu(II) and Ni(II) activation in the flotation of quartz, lizardite and chlorite. *International Journal of Mineral Processing*, *76*(1), 75-81. https://doi.org/https://doi.org/10.1016/j.minpro.2004.12.002

Fuerstenau, D. W., & Healy, T. W. (1972). CHAPTER 6 - PRINCIPLES OF MINERAL FLOTATION. In R. Lemlich (Ed.), *Adsorptive Bubble Separation Techniques* (pp. 91-131). Academic Press. https://doi.org/https://doi.org/10.1016/B978-0-12-443350-2.50011-3

Fuerstenau, M., & Cummins, W. (1967). The role of basic aqueous complexes in anionic flotation of quartz. *Trans. Aime*, *238*, 196.

Gaudin, A. M. (1939). Principles of mineral dressing.

Guo, W., Zhu, Y., Han, Y., Li, Y., & Yuan, S. (2020). Flotation performance and adsorption mechanism of a new collector 2-(carbamoylamino) lauric acid on quartz surface. *Minerals Engineering*, *153*, 106343. https://doi.org/https://doi.org/10.1016/j.mineng.2020.106343

Irannajad, M., Salmani Nuri, O., & Allahkarami, E. (2018). A new approach in separation process evaluation. Efficiency ratio and upgrading curves [journal article]. *Physicochemical Problems of Mineral Processing*, *54*(3), 847-857. https://doi.org/https://doi.org/10.5277/ppmp1886

Jie, Z., Weiqing, W., Jing, L., Yang, H., Qiming, F., & Hong, Z. (2014). Fe(III) as an activator for the flotation of spodumene, albite, and quartz minerals. *Minerals Engineering*, *61*, 16-22. https://doi.org/https://doi.org/10.1016/j.mineng.2014.03.004

Kar, B., Sahoo, H., Rath, S. S., & Das, B. (2013). Investigations on different starches as depressants for iron ore flotation. *Minerals Engineering*, *49*, 1-6. https://doi.org/https://doi.org/10.1016/j.mineng.2013.05.004

Kordloo, M., Khodadadmahmoudi, G., Ebrahimi, E., Rezaei, A., Tohry, A., & Chehreh Chelgani, S. (2023). Green hematite depression for reverse selective flotation separation from quartz by locust bean gum. *Scientific Reports*, *13*(1), 8980. https://doi.org/10.1038/s41598-023-36104-5

Kou, J., Xu, S., Sun, T., Sun, C., Guo, Y., & Wang, C. (2016). A study of sodium oleate adsorption on Ca2+ activated quartz surface using quartz crystal microbalance with dissipation. *International Journal of Mineral Processing*, *154*, 24-34. https://doi.org/https://doi.org/10.1016/j.minpro.2016.06.008

Luo, B., Zhu, Y., Sun, C., Li, Y., & Han, Y. (2015). Flotation and adsorption of a new collector α-Bromodecanoic acid on quartz surface. *Minerals Engineering*, *77*, 86-92. https://doi.org/https://doi.org/10.1016/j.mineng.2015.03.003

Luo, B., Zhu, Y., Sun, C., Li, Y., & Han, Y. (2018). The flotation behavior and adsorption mechanisms of 2-((2-(decyloxy) ethyl) amino) lauric acid on quartz surface. *Minerals Engineering*, *117*, 121-126.

Luo, B., Zhu, Y., Sun, C., Li, Y., & Han, Y. (2019). Molecular dynamic simulations study of 2-((2-(decyloxy) ethyl) amino) lauric acid adsorption on the α-quartz (1 0 1) surface. *Physicochemical Problems of Mineral Processing*, *55*.

Luo, B., Zhu, Y., Sun, C., Li, Y., & Han, Y. (2021). Reverse flotation of iron ore using amphoteric surfactant: 2-((2 (decyloxy) ethyl) amino) lauric acid. *Physicochemical Problems of Mineral Processing*, *57*. https://doi.org/https://doi.org/10.37190/ppmp/135441

Luo, X., Wang, Y., Wen, S., Ma, M., Sun, C., Yin, W., & Ma, Y. (2016). Effect of carbonate minerals on quartz flotation behavior under conditions of reverse anionic flotation of iron ores. *International Journal of Mineral Processing*, *152*, 1-6. https://doi.org/https://doi.org/10.1016/j.minpro.2016.04.008

Mensah, R., Perera, T. D. S., Hsia, T., Amani, P., Thang, S. H., & Firouzi, M. (2025). A Bio-Based Collector Derived from Vitamin E for Hematite Flotation. *Colloids and Interfaces*, *9*(2), 24.

Nakhaei, F., & Irannajad, M. (2018). Reagents types in flotation of iron oxide minerals: A review. *Mineral Processing and Extractive Metallurgy Review*, *39*(2), 89-124.

Ozkan, A., Ucbeyiay, H., & Duzyol, S. (2009). Comparison of stages in oil agglomeration process of quartz with sodium oleate in the presence of Ca(II) and Mg(II) ions. *Journal of Colloid and Interface Science*, *329*(1), 81-88. https://doi.org/https://doi.org/10.1016/j.jcis.2008.09.073

Parks, G. A. (1965). The Isoelectric Points of Solid Oxides, Solid Hydroxides, and Aqueous Hydroxo Complex Systems. *Chemical Reviews*, *65*(2), 177-198. https://doi.org/10.1021/cr60234a002

Quast, K. (2006). Flotation of hematite using C6–C18 saturated fatty acids. *Minerals Engineering*, *19*(6), 582-597. https://doi.org/https://doi.org/10.1016/j.mineng.2005.09.010

Rath, S. S., & Sahoo, H. (2022). A Review on the Application of Starch as Depressant in Iron Ore Flotation. *Mineral Processing and Extractive Metallurgy Review*, *43*(1), 122-135. https://doi.org/10.1080/08827508.2020.1843028

Sahoo, H., Rath, S., Jena, S., Mishra, B., & Das, B. (2015). Aliquat-336 as a novel collector for quartz flotation. *Advanced Powder Technology*, *26*(2), 511-518.

Tohry, A., Dehghan, R., de Salles Leal Filho, L., & Chehreh Chelgani, S. (2021). Tannin: An eco-friendly depressant for the green flotation separation of hematite from quartz. *Minerals Engineering*, *168*, 106917. https://doi.org/https://doi.org/10.1016/j.mineng.2021.106917

Turrer, H. D. G., & Peres, A. E. C. (2010). Investigation on alternative depressants for iron ore flotation. *Minerals Engineering*, *23*(11), 1066-1069. https://doi.org/https://doi.org/10.1016/j.mineng.2010.05.009

U.S Geological Survey, Minerals Commodity Summarise. (2023). Retrieved 10/03/2025 from https://pubs.usgs.gov/publication/mcs2023

Weissenborn, P. K., Warren, L. J., & Dunn, J. G. (1994). Optimisation of selective flocculation of ultrafine iron ore. *International Journal of Mineral Processing*, *42*(3), 191-213. https://doi.org/https://doi.org/10.1016/0301-7516(94)00026-3

Weissenborn, P. K., Warren, L. J., & Dunn, J. G. (1995). Selective flocculation of ultrafine iron ore 2. Mechanism of selective flocculation. *Colloids and Surfaces A: Physicochemical and Engineering Aspects*, *99*(1), 29-43. https://doi.org/https://doi.org/10.1016/0927-7757(95)03112-Q

Western Australia Mineral and Petroleum Statistics Digest 2022-23. (2024). online Retrieved from https://www.wa.gov.au/media/137381/download?inline

Wills, B. A., & Finch, J. (2015). *Wills' mineral processing technology: an introduction to the practical aspects of ore treatment and mineral recovery*. Butterworth-heinemann.

Wright, B., Amani, P., Galvin, K., & Firouzi, M. (2025). Mitigating the Adverse Effect of Salts on Gangue Recovery Using a Reflux Flotation Cell. *Mineral Processing and Extractive Metallurgy Review*, 1-14. https://doi.org/10.1080/08827508.2025.2502857

Wu, F., Cao, S., Yin, W., Fu, Y., Li, C., & Cao, Y. (2024). Improved Quartz Flotation at Low Temperature by Amino Acid Lauryl Lysine as a Novel Green Collector. *Minerals*, *14*(10), 972. https://doi.org/https://doi.org/10.3390/min14100972

Zhang, H., Lin, S., Guo, Z., Sun, W., & Zhang, C. (2023). Selective separation mechanism of hematite from quartz by anionic reverse flotation: Implications from surface hydroxylation. *Applied Surface Science*, *614*, 156056.

Zhu, Y., Luo, B., Sun, C., Li, Y., & Han, Y. (2015). Influence of bromine modification on collecting property of lauric acid. *Minerals Engineering*, *79*, 24-30. https://doi.org/https://doi.org/10.1016/j.mineng.2015.05.006